

See discussions, stats, and author profiles for this publication at: <https://www.researchgate.net/publication/370353762>

Thermal transport properties of nanoporous silicon with significant specific surface area

Article in *Applied Physics Letters* · April 2023

DOI: 10.1063/5.0148434

CITATIONS

4

READS

163

4 authors, including:



[Mykola Isaiev](#)

French National Centre for Scientific Research

122 PUBLICATIONS 985 CITATIONS

[SEE PROFILE](#)



[V. V. Kuryliuk](#)

Taras Shevchenko National University of Kyiv

66 PUBLICATIONS 285 CITATIONS

[SEE PROFILE](#)



[David Lacroix](#)

University of Lorraine

157 PUBLICATIONS 2,377 CITATIONS

[SEE PROFILE](#)

Thermal Transport Properties of Nanoporous Silicon with Significant Specific Surface Area

Mykola Isaiev^{1c}, Yuliia Mankovska^{2*}, Vasyl Kuryliuk², and David Lacroix¹

¹*Université de Lorraine, CNRS, LEMTA, Nancy F-54000, France*

²*Faculty of Physics, Taras Shevchenko National University of Kyiv, 64/13, Volodymyrska Str., 01601 Kyiv, Ukraine*

**Current affiliation: Laboratoire d'Optique Appliquée – ENSTA Paris, Ecole Polytechnique, CNRS, IP Paris, Palaiseau, France*

^cCorresponding author: mykola.isaiev@univ-lorraine.fr

This paper studies thermal transport in nanoporous silicon with a significant specific surface area. First, the equilibrium molecular dynamics approach was used to obtain the dependence of thermal conductivity on a specific surface area. Then, a modified phonon transport kinetic theory-based approach was developed to analyze thermal conductivity. Two models were used to evaluate the phonon mean free path in the porous materials. The first model assumes that the dependence of the mean free path only relies on the specific surface area, and the second one also considers the mean free path variation with the porosity. Both approaches approximate molecular dynamics data well for the smaller porosity values. However, the first model fails for highly porous matrixes, while the second one matches well with molecular dynamics simulations across all considered ranges of the porosities. This work illustrates that the phonon mean free path dependence with the porosity/volume fraction of composite materials is essential for describing thermal transport in systems with significant surface-to-volume fractions.

The miniaturization of electronic devices and their components nowadays leads to issues such as overheating with hotspots and subsequent failure occurrence. Therefore, further development of such technologies requires significant efforts to establish the background of efficient thermal management in nanostructured objects. The latter involves understanding heat carriers transfer mechanisms, scattering and interactions close to an interface separating different species. Porous silicon (PS) is an excellent candidate to be a model object to investigate various conditions favoring/disfavoring thermal transport ^{1,2}. From a practical point of view, one can fabricate PS with a wide range of pore sizes, porosity, and morphology³. Thus, it gives an excellent and clear basis for experimental verifications of the developed models^{4,5}. Further, such results can be broadcasted for various nanocomposite systems, where interfacial boundaries also crucially impact thermal transport^{6,7}.

Specifically, the significant reduction of thermal conductivity of PS compared to the bulk one is already well known^{8,9}. Two main reasons explain this: i) the natural removal of material and ii) the phonon scattering at the interfaces. The first mechanism arises due to the lowering of the number of energy

carriers per unit volume in the porous materials as compared to the bulk one. It results from material extraction by voids formation, and it is dominant for large pore radius. The second is more crucial while decreasing the pore radius while maintaining overall porosity volume, and thus increasing the phonon scattering specific surface area, i.e. the total interfacial area per system volume. A model that describes this tendency is Minnich and Chen model¹⁰. The latter describes the dependence of thermal conductivity of porous and composite systems. It has been used for a wide range of materials and broad volumetric fraction of pores or inclusion components^{11–13}.

In Minnich and Chen model, the effective thermal conductivity of a nanoporous system (λ) can be decomposed into multiplicands:

$$\lambda = \lambda_{nm} F, \quad (1)$$

where λ_{nm} is the thermal conductivity of the nanoporous matrix, which differs from the bulk one due to the phonons mean free path reduction as a result of the scattering on the interfacial boundaries; F is the factor describing the reduction of thermal conductivity due to the decrease the portion of the bulk material. According to the Maxwell model for effective media, this factor can be presented as follows for porous material¹⁴:

$$F = \frac{2 - 2P}{2 + P}, \quad (2)$$

where P is the porosity.

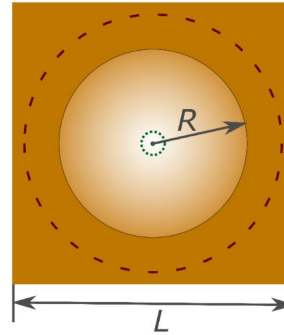


Fig. 1. Sketch view of the considered simulated domain. The minimum and maximum pore radii are characterized by dotted and dashed circles respectively. Here those radii correspond to the case $L = 12a$

Regarding the thermal conductivity of the nanoporous matrix, Minnich and Chen proposed a simple approach for the evaluation of the thermal conductivity of the matrix as follows:

$$\lambda_{nm} = \frac{1}{3} C_h v_h \frac{1}{1/\Lambda_h + \Phi/4}, \quad (3)$$

where C_h is the volumetric heat capacity of the host matrix, v_h is the mean velocity of phonons of the host matrix, Λ_h is the mean free path in the host matrix material, and $\Phi = \frac{A_{por}}{V_{box}}$ is the specific surface

area of the pore. Eq. (3) is based on several assumptions, and one of them is that the cross-section of the phonons' scattering at the pore edge has the following form:

$$\sigma = \pi R^2, \quad (4)$$

where R is the pore radius. This cross-section corresponds to the assumption of the phonon scattering at the edge of a solid sphere. Yet, this assumption forms the bottleneck of the approach and its application to the cases of small pore radii with a very high interface density, where the multiple scattering events are frequent.

Therefore, our work aims to understand the role of multi-scattering processes in the perturbation of heat transfer in nanoporous materials. We first simulated thermal conductivity in porous silicon using the equilibrium molecular dynamics (EMD) approach. Then, we adapted the kinetic theory (KT) approach to model thermal conductivity in PS, considering the contribution of each mode to heat transfer. The latter allows us to identify the role of different mechanisms leading to the modification of the thermal transport performance of the porous matrix.

In this work, we investigated a crystalline silicon matrix with a lattice constant equal to $a = 5.431 \text{ \AA}$ for molecular dynamics simulations; the simulation domains contain a repeated translation of silicon cells in x , y , and z directions. We chose the number of repetitions (n) to equal 6, 8, 10, and 12, and the domain size was $L = n a$. Periodic boundary conditions were set in all directions. Pore structure was created by cutting out the atoms in a sphere with a radius R located in the center of the simulated domain. The sphere radius was considered in the range from 0 (bulk silicon) to $(L - a)/2$ with the step $a/2$. Such variation of L and R allows us to consider porosity and specific area of nanoporous material in a wide range. The interaction between silicon atoms was simulated with the respect of Tersoff potential¹⁵.

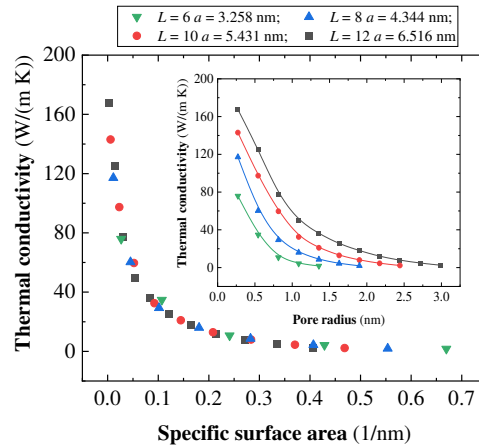


Fig. 2. Dependence of thermal conductivity with the specific surface ratio of a pore. Inset: Dependence of thermal conductivity with pore radius

We used the Green-Kubo formalism for the thermal conductivity calculations:

$$\lambda = \frac{1}{3Vk_B T} \int_0^{t_c} dt \langle \mathbf{J}(0) \mathbf{J}(t) \rangle_{t_s}, \quad (5)$$

where V is the volume of the simulation domain, T is the temperature, $\mathbf{J}(t)$ is the heat flux vector, t_c is the finite correlation time for which integration was carried out, t_s is the sampling time for sampling time over which the autocorrelation function was accumulated for averaging.

Fig. 2 presents the dependence of thermal conductivity with the pore specific surface area for different box sizes. The inset of Fig. 2 details the dependence of the thermal conductivity as a function of the pore radius. As shown in Fig. 2, the specific surface ratio is the more versatile parameter for describing thermal conductivity reduction in the considered pore radius range.

In order to evaluate the Minnich and Chen model¹⁰ for thermal transport in composite media, we used the kinetic theory (KT) approach developed previously by P. Chantrenne et al¹⁶. In the frames of this model, the thermal conductivity of the nanoporous matrix can be represented as follows:

$$\lambda_{nm} = 6 \frac{k_B}{3 \frac{a^3}{4}} \int_0^\infty d\omega C_V(\omega) D(\omega) \sum_p \xi(\omega, p) v^2(\omega, p) \tau(\omega, p), \quad (6)$$

where k_B is the Boltzmann constant, ω and p are the phonon frequency and the polarization, $C_V(\omega)$ is the per mode per unit volume heat capacity, $D(\omega)$ is the phonons density of states, $v(\omega, p)$ is the phonon group velocity, $\tau(\omega, p)$ is the phonon relaxation time due to phonons scattering, $\xi(\omega, p)$ is the coefficient to express the contributions of different polarizations to the phonons density of states.

Considering the classical nature of MD computations, we use the KT model with constant (high-temperature limit) heat capacity to minimize the number of different factors in KT and MD approaches. $D(\omega)$, $v(\omega, p)$ and $\xi(\omega, p)$ were taken from our previous paper¹⁷. According to the Matthiessen rule, the resulting relaxation time (RT) was calculated as follows

$$\tau^{-1}(\omega, p) = \tau_{ph-ph}^{-1} + \tau_{por}^{-1}, \quad (7)$$

where τ_{ph-ph} is the lifetime due to phonon-phonon scattering; this dependence was also taken from¹⁷; τ_{por} is the lifetime due to phonon scattering at the pore edge. In our calculations, we evaluate this lifetime as follows

$$\tau_{por} = \frac{l_{por}}{v(\omega, p)}, \quad (8)$$

where l_{por} is the mean free path due to phonon scattering at the pore edge. Following Minnich and Chen¹⁰, it was estimated as

$$l_{por} = l_{Minnich} = \frac{4}{\Phi} = \frac{L^3}{\pi R^2}. \quad (9)$$

Fig. 3 presents the dependence of the thermal conductivity of the nanoporous matrix calculated with the KT approach by Eq. (6) and the one evaluated from MD simulations by Eq. (1).

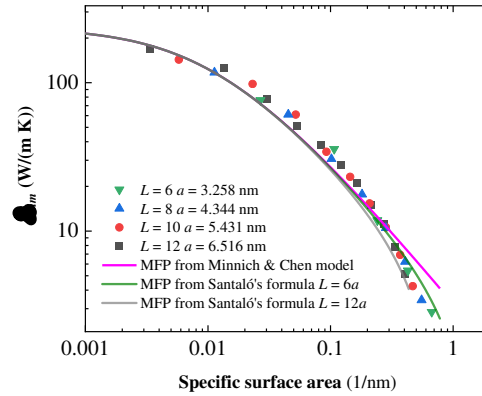


Fig. 3. The dependence of the thermal conductivity of the nanoporous matrix calculated with the KT and MD approaches

As shown in Fig. 3, the Minnich and Chen model approximates well MD data for the small and intermediate regions of specific surface area (before 0.3 nm^{-1}). While for the high interfacial density, the difference in thermal conductivity may reach 100%. Therefore, one can conclude that phonon localization may play a significant role in high interface densities. Such localization may arise as a result of decreasing distance between pores due to the necking effect^{18,19}. The distance decreases mainly because of the increased volume occupied by a pore.

In order to take this into account, we use the approximation of the mean free path obtained for the periodic Lorentz gas represented by two types of particles. The first type is the “heavy particles” periodically located in a 3d lattice representing the pores, while the “light particles” represent the phonons. For such a configuration, the mean free path of the light particle due to the scattering on heavy one can be represented by Santaló's formula^{20,21}:

$$l_{\text{Santaló}} = \frac{L^3 - \frac{4}{3}\pi R^3}{\pi R^2} = (1 - P)l_{\text{Minnich}}, \quad (10)$$

where P is the porosity. As one can see, Santaló's formula for the mean free path also shows the impact of reducing the material's volume on the mean free path. This impact is crucial for highly porous materials with an enormous specific surface area. One should note that Eq. (10) was obtained for specular scattering of the light particle at the surface of the heavy one (billiard model).

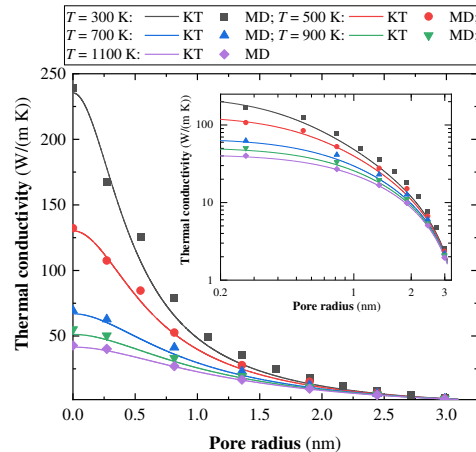


Fig. 4 Dependence of thermal conductivity with pore radius for different temperatures (the case $L = 12 a$)

The analytical description of the modified mean free path with Santaló's formula is also presented in Fig. 3. As one can see, this model well describes the dependence of thermal conductivity for higher values of the specific surface area. It should be noted that in Fig. 3, we presented the curve only for two extreme cases $L = 6a$ and $L = 12a$. As shown in Fig. 3, the impact of the volume reduction is more pronounced for the bigger box for the same specific surface area. However, the deviation of both curves from the one given by the Minnich and Chen approximation is significant only under the enormous specific surface area, which may arise only at the nanoscale.

The KT model with the mean free path modification based on the "billiard model" also describes the temperature dependence of porous silicon (see Fig. 4).

We want to stress that the impact of the porosity on the phonon mean free path in the current letter is demonstrated for a porous system made of a periodically arranged spherical pores network. Nevertheless, the core equations for KT modelling (Eq. (6) and Eq (7)) used here are quite general. Therefore, the results presented here can be broadcasted for different porous and composite systems, including non-periodical arrangements. Specifically, this approach can be easily adapted for the systems where mean free path can be obtained analytically (for example, for cylindrical or slit pore geometry) or numerically (for instance, with the use of Monte-Carlo approach to solve phonon Boltzmann Transport Equation^{22,23}).

In conclusion, we performed MD simulations and KT modelling of thermal conductivity in porous silicon for different specific surface areas. We found a significant reduction of TC for large specific surface ratio. In the latter case the prediction based on the Minnich and Chen model fails. Thus, Santaló's formula used to evaluate the mean free path in a Lorentz gas was adopted to approximate the mean free path in high porosity silicon. This formula considers the dependence of the mean free path with the porosity itself. Specifically, such dependence arises due to the necking effect – decreasing the distance between pores. The analytical KT model with the mean free path estimation by the Santaló's formula predicts well the variations of thermal conductivity for higher porosity. Thus, we can state the crucial impact of the volume

fraction of the composite components at the nanoscale on the phonon mean-free reduction. The latter should be considered for thermal engineering in nanoelectronics, where the components' size is currently trending to several nanometers²⁴.

Acknowledgment.

This paper contains the results obtained in the frames of the projects "Hotline" ANR-19-CE09-0003 and "FASTE" ANR-22-CE50-002. This work was performed using HPC resources from GENCI-TGCC and GENCI-IDRIS (A0130913052), in addition HPC resources were partially provided by the EXPLOR center hosted by the Université de Lorraine. Thanks to "STOCK NRJ" that is co-financed by the European Union within the framework of the Program FEDER-FSE Lorraine and Massif des Vosges 2014–2020.

¹ M. Isaiev, X. Wang, K. Termentzidis, and D. Lacroix, "Thermal transport enhancement of hybrid nanocomposites; impact of confined water inside nanoporous silicon," *Appl Phys Lett* **117**(3), 033701 (2020).

² R. Vercauteren, G. Scheen, J.P. Raskin, and L.A. Francis, "Porous silicon membranes and their applications: Recent advances," *Sens Actuators A Phys* **318**, (2021).

³ R.F. Sierra-Moreno, I.A. Lujan-Cabrera, J.M. Cabrera-Teran, E. Ortiz-Vazquez, M.E. Rodriguez-Garcia, and C.F. Ramirez-Gutierrez, "Study of the optical response of oxidized porous silicon structures by thermal oxidation in air," *J Mater Sci* **57**(24), 11226–11241 (2022).

⁴ C.F. Ramirez-Gutierrez, J.D. Castaño-Yepes, and M.E. Rodriguez-García, "In situ photoacoustic characterization for porous silicon growing: Detection principles," *J Appl Phys* **119**(18), 185103 (2016).

⁵ K. Dubyk, T. Nychporuk, V. Lysenko, K. Termentzidis, G. Castanet, F. Lemoine, D. Lacroix, and M. Isaiev, "Thermal properties study of silicon nanostructures by photoacoustic techniques," *J Appl Phys* **127**(22), 225101 (2020).

⁶ V. Kuryliuk, O. Tyvonovych, and S. Semchuk, "Impact of Ge clustering on the thermal conductivity of SiGe nanowires: atomistic simulation study," *Physical Chemistry Chemical Physics* **25**(8), 6263–6269 (2023).

⁷ O. Makukha, I. Lysenko, and A. Belarouci, "Liquid-Modulated Photothermal Phenomena in Porous Silicon Nanostructures Studied by μ -Raman Spectroscopy," *Nanomaterials* **13**(2), 310 (2023).

⁸ S. Erfantalab, P. Sharma, G. Parish, and A. Keating, "Thermal analysis of surface micromachined porous silicon membranes using the 3 ω method: Implications for thermal sensing," *Appl Therm Eng* **222**(October 2022), 119965 (2023).

⁹ N. Koshida, *Thermal Properties of Nanoporous Silicon Materials*, 2nd ed. (Elsevier Ltd., 2021).

¹⁰ A. Minnich, and G. Chen, "Modified effective medium formulation for the thermal conductivity of nanocomposites," *Appl Phys Lett* **91**(7), 073105 (2007).

¹¹ T.W. Pfeifer, J.A. Tomko, E. Hoglund, E.A. Scott, K. Hattar, K. Huynh, M. Liao, M. Goorsky, and P.E. Hopkins, "Measuring sub-surface spatially varying thermal conductivity of silicon implanted with krypton," *J Appl Phys* **132**(7), (2022).

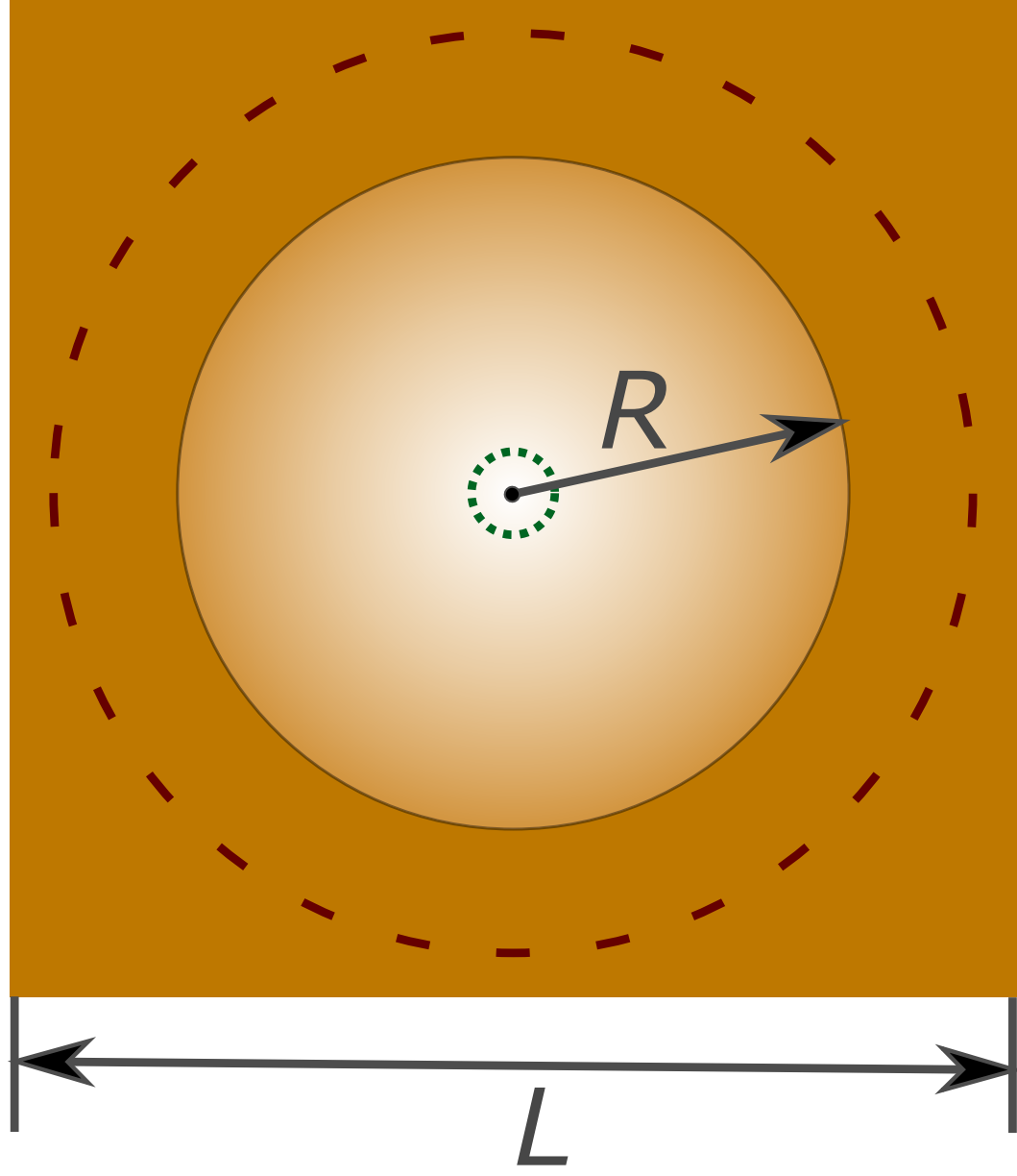
This is the author's peer reviewed, accepted manuscript. However, the online version of record will be different from this version once it has been copyedited and typeset.

PLEASE CITE THIS ARTICLE AS DOI: 10.1063/5.0148434

- ¹² V.C.S. Theja, V. Karthikeyan, D.S. Assi, and V.A.L. Roy, "Insights into the Classification of Nanoinclusions of Composites for Thermoelectric Applications," *ACS Appl Electron Mater* **4**(10), 4781–4796 (2022).
- ¹³ V. Jean, S. Fumeron, K. Termentzidis, S. Tutashkonko, and D. Lacroix, "Monte Carlo simulations of phonon transport in nanoporous silicon and germanium," *J Appl Phys* **115**(2), 024304 (2014).
- ¹⁴ C.W. Nan, R. Birringer, D.R. Clarke, and H. Gleiter, "Effective thermal conductivity of particulate composites with interfacial thermal resistance," *J Appl Phys* **81**(10), 6692–6699 (1997).
- ¹⁵ J. Tersoff, "Modeling solid-state chemistry: Interatomic potentials for multicomponent systems," *Phys Rev B* **39**(8), 5566–5568 (1989).
- ¹⁶ P. Chantrenne, J.L. Barrat, X. Blase, and J.D. Gale, "An analytical model for the thermal conductivity of silicon nanostructures," *J Appl Phys* **97**(10), 104318 (2005).
- ¹⁷ V. Kuryliuk, O. Nepochaty, P. Chantrenne, D. Lacroix, and M. Isaiev, "Thermal conductivity of strained silicon: Molecular dynamics insight and kinetic theory approach," *J Appl Phys* **126**(5), 055109 (2019).
- ¹⁸ P. Chantrenne, and V. Lysenko, "Thermal conductivity of interconnected silicon nanoparticles: Application to porous silicon nanostructures," *Phys Rev B* **72**(3), 035318 (2005).
- ¹⁹ M. Nomura, R. Anufriev, Z. Zhang, J. Maire, Y. Guo, R. Yanagisawa, and S. Volz, "Review of thermal transport in phononic crystals," *Materials Today Physics* **22**, 100613 (2022).
- ²⁰ S.A. Santaló, "Sobre la distribución probable de corpúsculos en un cuerpo, deducida de la distribución en sus secciones y problemas análogos," *Revista de La Unión Matemática Argentina* **IX**(5), 145–164 (1943).
- ²¹ F. Golse, in *Nonlinear Partial Differential Equations*, edited by X. Cabré, and J. Soler, Advanced C (Springer Basel, Barcelona, 2012), pp. 39–99.
- ²² Y. Suzuki, Y. Fujita, K. Fauziah, T. Nogita, H. Ikeda, T. Watanabe, and Y. Kamakura, in *2020 International Conference on Simulation of Semiconductor Processes and Devices (SISPAD)* (IEEE, 2020), pp. 15–18.
- ²³ M. Sledzinska, B. Graczykowski, F. Alzina, U. Melia, K. Termentzidis, D. Lacroix, and C.M. Sotomayor Torres, "Thermal conductivity in disordered porous nanomembranes," *Nanotechnology* **30**(26), 265401 (2019).
- ²⁴ IBM, "IBM Unveils World's First 2 Nanometer Chip Technology, Opening a New Frontier for Semiconductors," <https://Newsroom.Ibm.Com/2021-05-06-IBM-Unveils-Worlds-First-2-Nanometer-Chip-Technology,-Opening-a-New-Frontier-for-Semiconductors>, (2021).

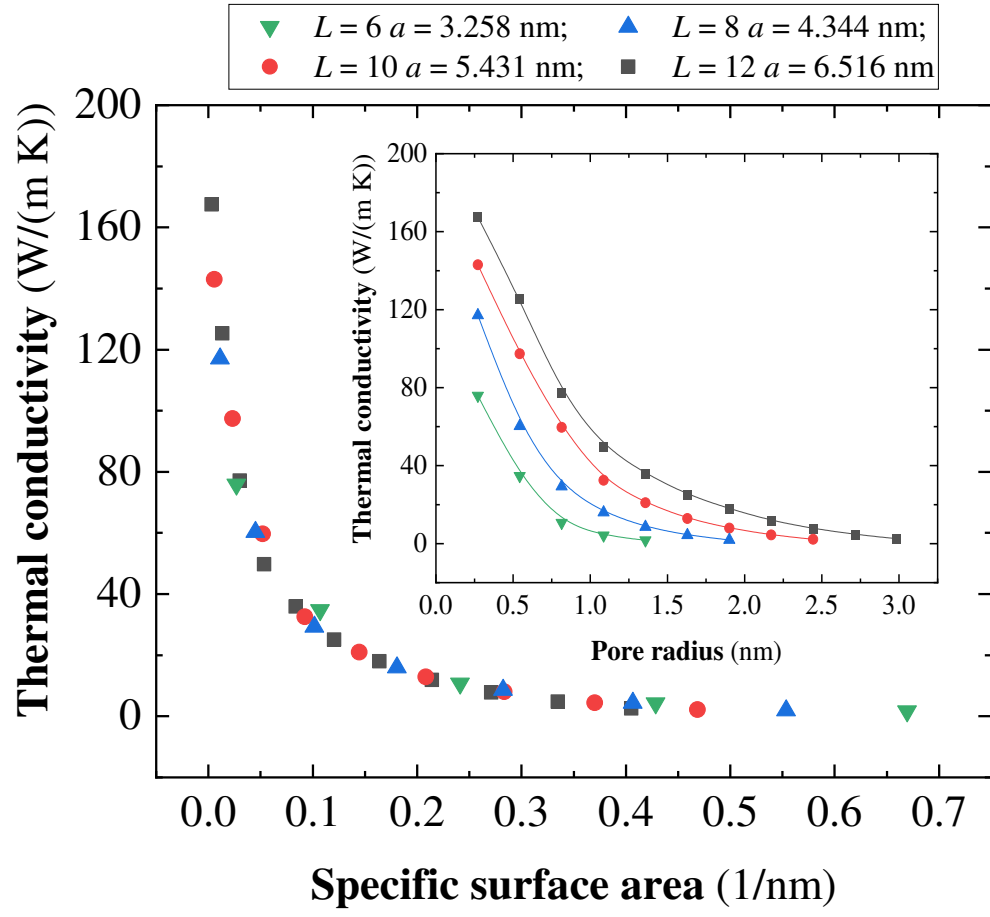
This is the author's peer reviewed, accepted manuscript. However, the online version of record will be different from this version once it has been copyedited and typeset.

PLEASE CITE THIS ARTICLE AS DOI: 10.1063/5.0148434



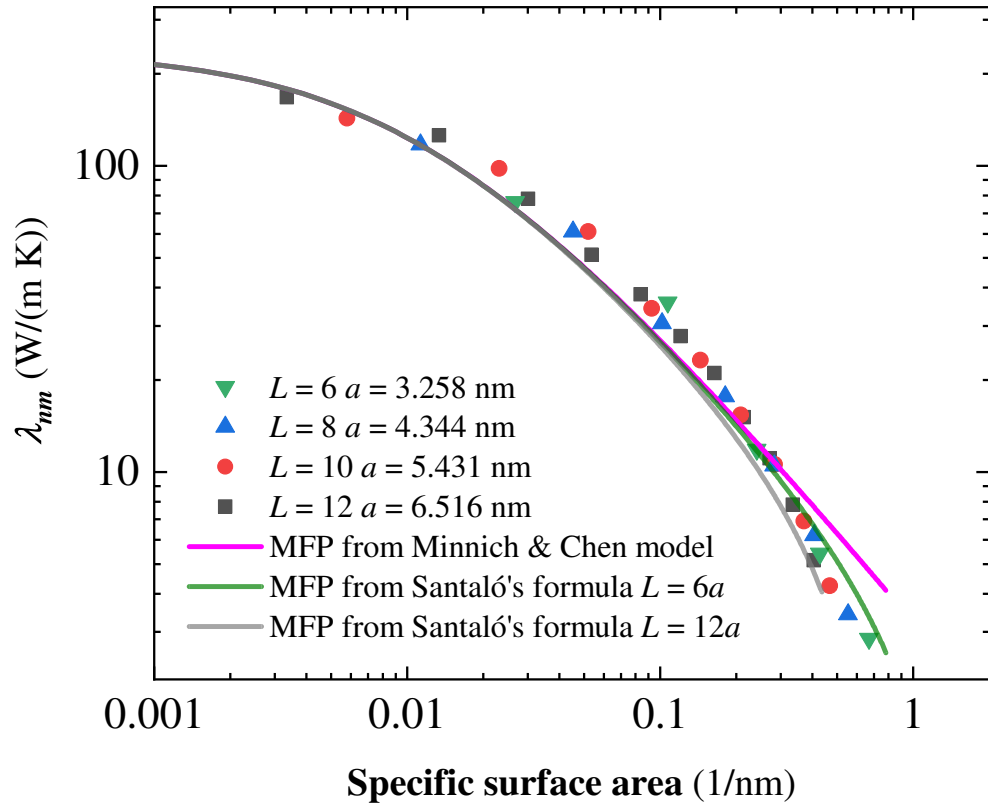
This is the author's peer reviewed, accepted manuscript. However, the online version of record will be different from this version once it has been copyedited and typeset.

PLEASE CITE THIS ARTICLE AS DOI: 10.1063/5.0148434



This is the author's peer reviewed, accepted manuscript. However, the online version of record will be different from this version once it has been copyedited and typeset.

PLEASE CITE THIS ARTICLE AS DOI: 10.1063/5.0148434



This is the author's peer reviewed, accepted manuscript. However, the online version of record will be different from this version once it has been copyedited and typeset.

PLEASE CITE THIS ARTICLE AS DOI: 10.1063/5.0148434

